Published in final edited form as:
Proc IEEE Int Symp Biomed Imaging. 2011 December 31; 2011: 1039–1043. doi:10.1109/ISBI.2011.5872579.

PRACTICAL PARALLEL IMAGING COMPRESSED SENSING MRI: SUMMARY OF TWO YEARS OF EXPERIENCE IN ACCELERATING BODY MRI OF PEDIATRIC PATIENTS

SS Vasanawala[2], **MJ Murphy**[1], **MT Alley**[2], **P Lai**[3], **K Keutzer**[1], **JM Pauly**[4], and **M Lustig**[1]

[1]Electrical Engineering and Computer Science, University of California, Berkeley

[2]Radiology, Stanford University

[3]GE Healthcare

[4]Electrical Engineering, Stanford University

Abstract

For the last two years, we have been experimenting with applying compressed sensing parallel imaging for body imaging of pediatric patients. It is a joint-effort by teams from UC Berkeley, Stanford University and GE Healthcare. This paper aims to summarize our experience so far. We describe our acquisition approach: 3D spoiled-gradient-echo with poisson-disc random undersampling of the phase encodes. Our re-construction approach: ℓ_1-SPIRiT, an iterative autocalibrating parallel imaging reconstruction that enforces both data consistency and joint-sparsity in the wavelet domain. Our implementation: an on-line parallelized implementation of ℓ_1-SPIRiT on multi-core CPU and General Purpose Graphics Processors (GPGPU) that achieves sub-minute 3D reconstructions with 8-channels. Clinical results showing higher quality reconstruction and better diagnostic confidence than parallel imaging alone at accelerations on the order of number of coils.

Index Terms

Compressed Sensing; Parallel Imaging; SPIRiT; Pediatric MRI

1. INTRODUCTION

Magnetic resonance (MR) imaging offers superb soft-tissue characterization with global anatomic assessment, has no ionizing radiation, and, thus, has the potential to be a dominant pediatric imaging modality [1]. However, a major limitation of MR imaging is slow imaging speed relative to computed tomography (CT). The resulting motion artifacts and frequent need for anesthesia often result in preference by radiologists and referring clinicians for CT, given its relative ease of use and robustness.

For the last two years we have been experimenting with accelerating acquisitions of pediatric body MRI using the combination of compressed sensing and parallel imaging. Our aim is to achieve fast and robust pediatric MRI that will reduce the need for general anesthesia in pediatric patients and make MRI a viable alternative to CT. This paper aims to describe our experience with compressed sensing in clinical practice. We describe our acquisition approach, reconstruction methods, implementation and results in clinical settings.

2. APPROACH

At first, our initial efforts were focussed on compressed sensing MRI alone [2]. In the last several years, our approach was to combine compressed sensing with a robust coil-by-coil autocalibrating parallel imaging (acPI) reconstruction[3]. A successful CS reconstruction has three main requirements: (i) sparsity of representation, (ii) incoherent sampling, and (iii) non-linear sparsity enforcing reconstruction. In order to synergistically combine CS with parallel imaging, we reconsidered these requirements in the context of (acPI) and proposed: a modified sparsity model for multiple coil images, an incoherent sampling scheme for imaging with multiple receivers, and an acPI reconstruction that exploits both imaging with multiple coils and the sparsity information. The acPI method is SPIRiT [4] which is based on self-consistency with the calibration and data acquisition. It is a method that exhibits higher accuracy and better noise performance than GRAPPA[5]. It supports arbitrary sampling, and provides a framework to incorporate sparsity constraints, which is essential for combination with CS.

2.1. Incoherent Sampling

In general, random sampling of *k*-space provides the high degree of incoherence needed for compressed sensing. However, pure random sampling is not optimized for parallel imaging with multiple receivers. Random sampling tends to produce sampling patterns with either large gaps or bunched samples. With multiple coil imaging, close samples in *k*-space are naturally correlated. This correlation enables the recovery of missing samples in parallel imaging. This means that bunched samples are “wasteful” as they provide little additional information on the signal. On the other hand, large gaps reduce the reconstruction conditioning of the parallel imaging. Random sampling with minimum distance between samples is called Poisson-disc sampling [6]. Sampling according to a Poisson-disc distribution provides high degree of incoherence and at the same time uniform distance between samples. In addition, this approach also provides flexibility for fractional and anisotropic acceleration (using ellipsoids rather than discs), resulting in a better fit to different coil array geometries.

2.2. Sparsity of Multiple Coils

The individual coil images are sensitivity weighted images of the original image of the magnetization. Edges in these images appear in the same spatial position, and therefore coefficients of sparse transforms, such as wavelets, exhibit similar sparsity patterns. To exploit this, we use a joint-sparsity model. In compressed sensing, sparsity is enforced by minimizing the ℓ_1-norm of a transformed image. The usual definition of the ℓ_1-norm is the sum of absolute values of all the transform coefficients, $\sum_c \sum_r |w_{cr}| = \sum_c \sum_r \sqrt{|w_{rc}|^2}$, where c is the coil index and *r* is the spatial index. In a joint-sparsity model we would like to jointly penalize coefficients from different coils that are at the same spatial position. Therefore we define a joint ℓ_1 as: $\mathrm{Joint}\ell_1(w) = \sum_r \sqrt{\sum_c |w_{rc}|^2}$. In a joint ℓ_1-norm model, the existence of large coefficient in one of the coils, protects the coefficients in the rest of the coils from being suppressed by the non-linear reconstruction.

2.3. ℓ_1-SPIRiT

SPIRiT is an autocalibrating parallel imaging reconstruction method. It is a generalization of GRAPPA. In SPIRiT, an interpolation kernel, *G*, is calibrated from a fully sampled calibration area in the center of k-space. The missing k-space samples are reconstructed such that they are consistent with the interpolator and the acquired data. Let *x* be the desired full *k*-space for all coils, *y* the acquired *k*-space, *D* be an operator that chooses acquired *k*-space

points out of the entire grid, then SPIRiT solves for x that satisfies both $Gx = x$ and $Dx = y$. To combine SPIRiT with CS we also require that the solution has a small Jointℓ_1-norm [7, 8]. Therefore we solve for,

$$\begin{aligned} \text{minimize} \quad & \text{Joint}\ell_1(\Psi x) \\ \text{s.t.} \quad & Gx = x \\ & Dx = y. \end{aligned} \tag{1}$$

3. IMPLEMENTATION

3.1. Pulse Sequence and Sampling

A standard three-dimensional (3D) spoiled gradient-recalled acquisition in the steady state sequence (SPGR) was modified to include a Poisson disc undersampling distribution of the phase-encodes. The advantage of the Poisson-disk sampling is that data can be reconstructed by using product parallel imaging reconstruction, such as autocalibrating reconstruction for cartesian sampling (ARC; GE Healthcare) [9], a variant of GRAPPA. The resulting images are more immune to calibration error, as any residual aliasing will be incoherent. This ability acts as a "safety net" when testing in patients. Our poisson-disc implementation is based on the algorithms described in http://www.devmag.org.za/articles/55-POISSON-DISK-SAMPLING/ and is based on the algorithm in [6]. The algorithm was modified to enable variable density [2] poisson-disc for better CS reconstruction and support for poisson-ellipse for supporting unisotropic accelerations. For simplicity of the reconstruction, the poisson-disc points that are generated are gridded to the closest grid point, and lie on a Cartesian grid. For large matrix size and high-acceleration the properties of the poisson-disc are fully preserved. For smaller size matrix and low-acceleration they are only approximate. In all the acquisitions a fully sampled window of at least 24 × 20 are acquires for the purpose of autocalibration.

3.2. ℓ_1-SPIRiT Implementation

To implement the optimization problem in Eq. (1) we chose a projection over convex sets (POCS) approach. This is an effective implementation that requires very simple operations: convolutions, Fourier and Wavelet transforms and soft-thresholding. The algorithm is the following:

1. Preparations:
   - i Normalize the scale of the data
   - i Calibrate a 3D kernel from autocalibration lines in 3D *k*-space
   - ii Compute an inverse Fourier transform of the data in the readout direction to create many separable 2D problems.
2. For each readout position:
   - i. Compute a 2D kernel, G, for the current readout position from the 3D kernel.
   - ii. Initialize: $x_0 = 0$, λ = "big"
   - iii. SPIRiT:

     Compute $x_{i+1} = Gx_i$
   - iv. CS Joint ℓ_1 Projection:

     $x_{i+1} = \Psi^{-1}$ JointSoftThresh(Ψx_{i+1}, λ)

v. Data consistency:

$$x_{i+1} = (I - D^T D)x_{i+1} + D^T y$$

vi. Adjust λ, Repeat iii–v

The JointSoftThresh operation is applied at each wavelet coefficient location. At each location is operates jointly on the coefficients from all coils. It computes:

$$\text{JointSoftThres}(w, \lambda) = w/\|w\| \cdot \{\|w\| - \lambda\}_+.$$

There are several implementation details that are worth noting: a) Since the readout direction is fully sampled, we compute the inverse Fourier transform and work on many separable 2D reconstruction problems. This reduces the complexity, simplifies the implementation and is easy to parallelize. b) The acquired data is unchanged. The algorithm is only used to extrapolate missing data in *k*-space. We have found that in doing so we consistently get better depiction of features and more natural looking images at the expense of slightly increasing noise. c) We use continuation of the soft-thresholding parameter from high penalty to a very low penalty. This often leads to much faster convergence of the iterations. We also found that radiologists prefer that images are not denoised. Therefore the ℓ_1-norm penalty is set such that minimal final denoizing is performed. d) Using orthogonal wavelets often results in some blocky artifacts. To mitigate this we use randomized shifting before the wavelet thresholding to approximate translation invariant wavelets as suggested by []. We have found that this approach significantly reduces the artifacts and produces much better diagnostic quality images.

3.3. Parallel Processing

The ℓ_1-SPIRiT POCS algorithm is very effective: it produces high-quality images usually after 50–100 iterations. Surprisingly, it is also relatively fast, in that it requires a very small number of operations: each iteration requires 2 (forward and inverse) Fourier Transforms, the SPIRiT *k*-space convolution operator is implemented cheaply as element-wise multiplication in the image domain, 2 Wavelet transforms (forward and inverse), and a very fast joint soft-threshold operation. Despite this inherent efficiency, the algorithm is still far more expensive than non-iterative reconstruction algorithms. However, we have demonstrated that the algorithm is very amenable to a massively parallel implementation [10].

We have implemented the POCS algorithm in both OpenMP and Nvidia's Cuda, and deployed it for on-line reconstructions on a dual-socket six-core 2.67 GHz Intel Westmere system with four Nvidia Tesla C1060's. The calibration implementation relies on Lapack [http://www.netlib.org/lapack] routines from AMD's ACML [http://www.amd.com/acml]. The POCS iterations are the more expensive step of the reconstruction, accounting typically for 95% of the runtime. As mentioned above, we decouple the 3D reconstruction into many independent 2D problems by inverse Fourier transforming along the fully sampled readout dimension. Both our OpenMP and our Cuda implementation execute multiple 2D problems in parallel. OpenMP executes each 2D reconstruction as a task, and we have as many 2D problems in flight simultaneously as there are CPU cores. Our deployed Cuda implementation concurrently solves as many 2D problems as there are GPUs in the system.[1] Within each 2D problem, we leverage vector-parallelism within the Fourier, Wavelet, interpolation, and thresholding operations to parallelize among thread blocks and threads

[1]Our next release concurrently solves as many 2D problems as there are Streaming Multiprocessors in the system's GPUs.

within a GPU. Efficient utilization of memory bandwidth is crucial to high performance, and wherever possible our implementation coalesces DRAM accesses and caches data in the GPU's scratchpad (shared) memories.

This parallel implementation provides clinically-useful runtimes of the efficient POCS ℓ_1-SPIRiT algorithm. Figure 2 shows the runtime of the Cuda POCS implementation running on the four GPUS in our recon system. Even for the largest dataset, which is representative of our highest-resolution scans on 32-channel coils, the POCS iterations run for less than 3 minutes. For typically sized 8-channel scans, runtimes are typically 30 seconds or less. Note that the Tesla C1060 GPUs in our current reconstruction machine are almost two years old: the reconstruction may run up to twice as fast on newer, Fermi-class GPUs.

3.4. Clinical Applications

Our CS 3D SPGR sequence was installed first on a 1.5T GE HDxt scanner and later on a 3T GE MR750. We first focused on applications that did not require intravenous contrast so that acceleration limits of the sequence could be explored by repeated acquisitions. These included whole brain imaging, and with the addition of fat suppression, volumetric cartilage imaging. The speed of the reconstruction facilitated iterative image acquisition, image evaluation, and parameter adjustments. We found we could double our imaging speed while maintaining diagnostic image quality [7].

The next application that we explored was magnetic resonance cholangiopancreatography (MRCP). MRCP exams are focused on the bile ducts of the liver and the duct that drains pancreatic fluids into the bowel. These ducts are rather small, filled with fluid that has a long T1 and T2 relaxation time, and are moving due to respiration. Thus, we sought to accelerate the MR acquisition such that high resolution could be maintained, but the scan completed in a breath-hold.

Thus, we modified our SPGR sequence to fully refocus magnetization in each repetition interval, yielding a sequence with T2/T1 contrast. In this case, the bile ducts are bright, but the remainder of human tissue for the most part is flat in contrast. Thus, this application is well suited to compressed sensing: sparse images, a pressing need for encoding speed, and inherent contrast such that acquisition could be repeated in an individual to optimize the technique. With this approach, we found we could achieve acceleration factors in excess of six, obtaining isotropic submillimeter resolution of the upper abdomen in a breath-hold.

We then turned attention to MRI exams enhanced with intravenous contrast. Here the introduction of new techniques is more challenging, as contrast may only be given once and has a rapid transit through the circulatory system. Therefore, only one acquisition can be obtained. Further, it has to be obtained in a manner that ensures high quality diagnostic images with no chance of compromising patient care. In this case, we focused our efforts on magnetic resonance angiography (MRA). Here again, small vessels have to be delineated rapidly, both for breath-holding, and now also because intravenous contrast has a short vascular residence time. Further, the application is similar to MRCP, as the images are relatively sparse, containing vessels and a flat background.

Our initial MRA exams were performed in patients who needed intravenous contrast for delayed contrast-enhanced imaging, but not MRA. This experience revealed that a doubling of imaging speed could be obtained with good image quality, or alternatively, higher resolution images could be obtained in the same scan time. Thus, we now routinely employ CS in our MRA exams. For children in whom a long breath-hold is a challenge, CS enables speed. For others, higher resolution is obtained.

4. EXPERIMENTS AND RESULTS

We recently performed a study in which 34 pediatric patients who required an MRI as part of their routine clinical care were enrolled. For these patients, scans were performed with an eight channel coil and at double to triple the speed we would ordinarily employ in routine clinical practice using traditional reconstruction methods. Images were were reconstructed with routine parallel imaging algorithm as well as with ℓ_1-SPIRiT and then presented to two radiologists to compare image quality and delineation of various anatomic structures. ℓ_1-SPIRiT image quality was consistently rated the same as or better than that of parallel imaging image quality (Wilcoxon and symmetry tests, $p < .001$), and this effect was strongest for those cases with higher accelerations. A reassuring result was that out of 325 structures evaluated, no structure was suppressed by the ℓ_1-SPIRiT reconstruction. Further, for half of the structures, radiologists preferred the ℓ_1-SPIRiT images, and 89 structures had increased degree of delineation with ℓ_1-SPIRiT.

While the preceding results were acquired at 1.5 Tesla field strength and eight-channel coils, the technical advances in reconstruction speed have permitted clinical deployment at 3 Tesla field strength with 32-channel coils. As children have smaller size than adults, the higher signal at 3 Tesla and with higher density receive coils greatly improves ability to resolve small anatomic structures. An example is shown in Figure 3. Figure 4 shows an example of a state-of-the art reconstruction with 32 channels and an even higher 8-fold acceleration.

5. CONCLUSION

We have presented a simple and effective approach to combining parallel imaging and compressed sensing. We have implemented a clinical pulse sequence and a fast on-line compressed sensing parallel imaging reconstruction. These are installed at Lucile Packard Children's Hospital and have been used clinically. Our results and experience show that the combination of compressed sensing and autocalibrated imaging is indeed feasible in a clinical setting. The solution presented above requires a small investment in additional computer hardware, but enables faster and/or higher resolution MRI compared to parallel imaging alone. This approach is of great value for pediatric imaging, but can be used in many other applications.

Acknowledgments

The authors are grateful for the support of GE Healthcare, the John and Tashia Morgridge Foundation, and the NIH (R01-EB009690, RR09794-15).

References

1. Olsen OE. Imaging of abdominal tumours: CT or MRI? Pediatr Radiol. 2008; 38(Suppl 3):S452–S458. [PubMed: 18470454]
2. Lustig, Michael; Donoho, David; Pauly, John M. Sparse MRI: The application of compressed sensing for rapid MR imaging. Magn Reson Med. Dec; 2007 58(6):1182–95. [PubMed: 17969013]
3. Blaimer, Martin; Breuer, Felix; Mueller, Matthias; Heidemann, Robin M.; Griswold, Mark A.; Jakob, Peter M. SMASH, SENSE, PILS, GRAPPA: how to choose the optimal method. Top Magn Reson Imaging. Aug; 2004 15(4):223–36. [PubMed: 15548953]
4. Lustig M, Pauly JM. SPIRiT: Iterative self-consistent parallel imaging reconstruction form arbitrary k-space. Magn Reson Med. 2010; 64(2):457–571. [PubMed: 20665790]
5. Griswold, Mark A.; Jakob, Peter M.; Heidemann, Robin M.; Nittka, Mathias; Jellus, Vladimir; Wang, Jianmin; Kiefer, Berthold; Haase, Axel. Generalized auto-calibrating partially parallel acquisitions (GRAPPA). Magn Reson Med. Jun; 2002 47(6):1202–10. [PubMed: 12111967]
6. Bridson R. Fast poisson disk sampling in arbitrary dimensions. ACM SIGGRAPH 2007. 2007

7. Vasanawala SS, Alleyadn MT, Hargreaves BA, Barth RA, Pauly JM, Lustig M. Improved pediatric MR imaging with compressed sensing. Radiology. 2010; 256(2):607–616. [PubMed: 20529991]

8. Lustig, Michael; Alley, Mark T.; Vasanawala, Shreyas; Donoho, David; Pauly, John. ℓ_1-SPIRiT: Autocalibrating parallel imaging compressed sensing. Proceedings of the 17th Annual Meeting of ISMRM; Honolulu, Hawaii. 2009. p. 379

9. Beatty, P.; Brau, A.; Chang, S.; Joshi, SM.; Michelich, CR.; Bayaram, E.; Netlson, TE.; Herfkens, R.; Brittain, JH. A method for autocalibrating 2-d accelerated volumetric parallel imaging with clinically practical reconstruction times. Proceedings of the 15th Annual Meeting of ISMRM; Berlin, Germany. 2007. p. 1749

10. Murphy, Mark; Keutzer, Kurt; Vasanawala, Shreyas; Lustig, Michael. Clinically feasible reconstruction time for ℓ_1-spirit parallel imaging and compressed sensing MRI. Proceedings of the 18th Annual Meeting of ISMRM; Stockhold, Sweeden. 2010. p. 4854

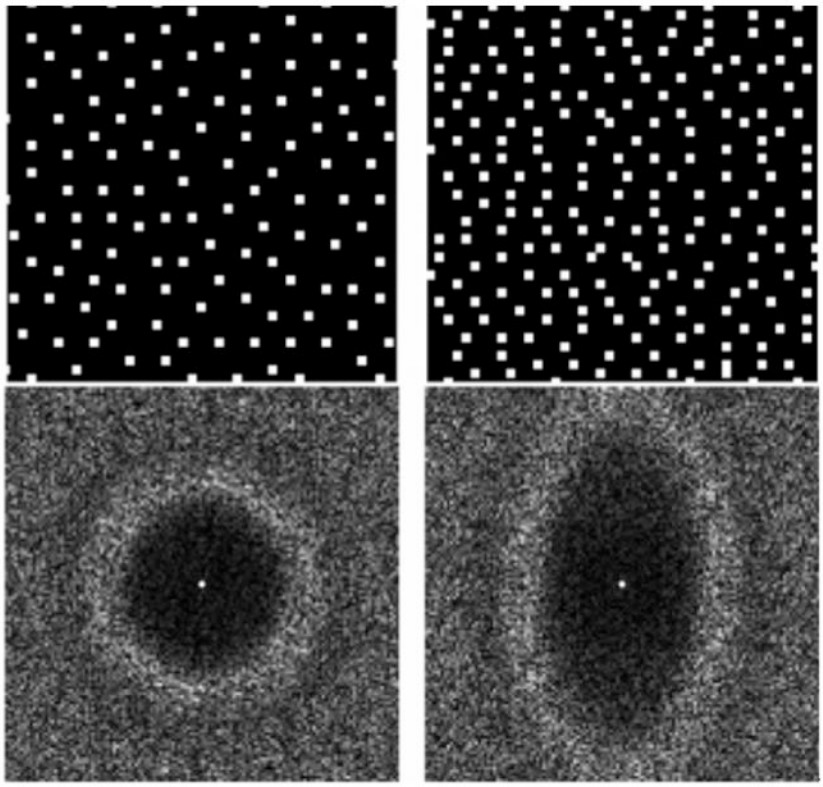

Fig. 1.
An example of a 4x4 and a 2.2x4.3 2D accelerated Poisson disc sampling patterns and their associated point spread functions. The incoherent aliasing appears beyond the Nyquist-rate supported field of view. Non-isotropic FOV can be used to adapt to coil array geometries.

Matrix Size	POCS Runtime
172x230x188x32	169.9 s
192x320x110x32	120.7 s
320x206x108x12	59.3s
192x320x66x8	24.4 s

Fig. 2.
ℓ_1-SPIRiT POCS runtime for four representative scans: two large 32-channels, a high-resolution 12-channel scan, and a smaller 8-channel scan.

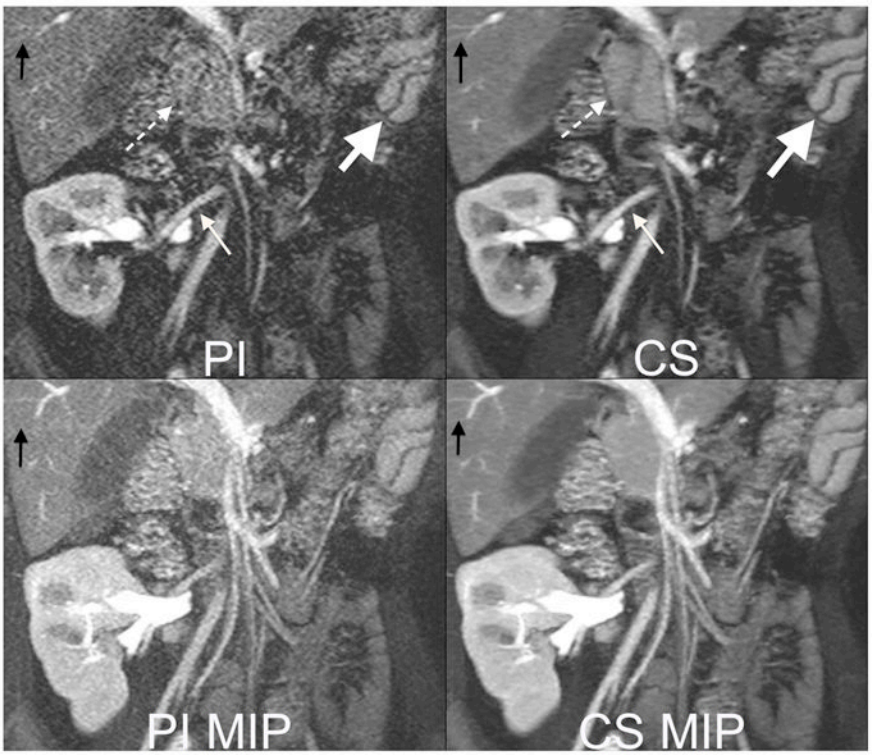

Fig. 3.

6 year old female with a transplanted kidney. Top: Cropped images from a 13 second 3 Tesla acquisition with 32 channels and an acceleration factor of 6. The high acceleration factor permits 320x320 matrix with 2 mm slice thickness. Note improved delineation of artery to the kidney (small white arrow), head of the pancreas (dashed arrow), small vessels in the liver (black arrow) with compressed sensing (CS) reconstruction than parallel imaging (PI) reconstruction. The fast acquisition also permits capturing fast perfusion dynamics, as seen by the differences in contrast enhancement of the splenic red and white pulp tissues (big white arrow). Bottom: Maximum intensity projections (MIP) highlight improved image quality with decreased noise afforded by the CS reconstruction.

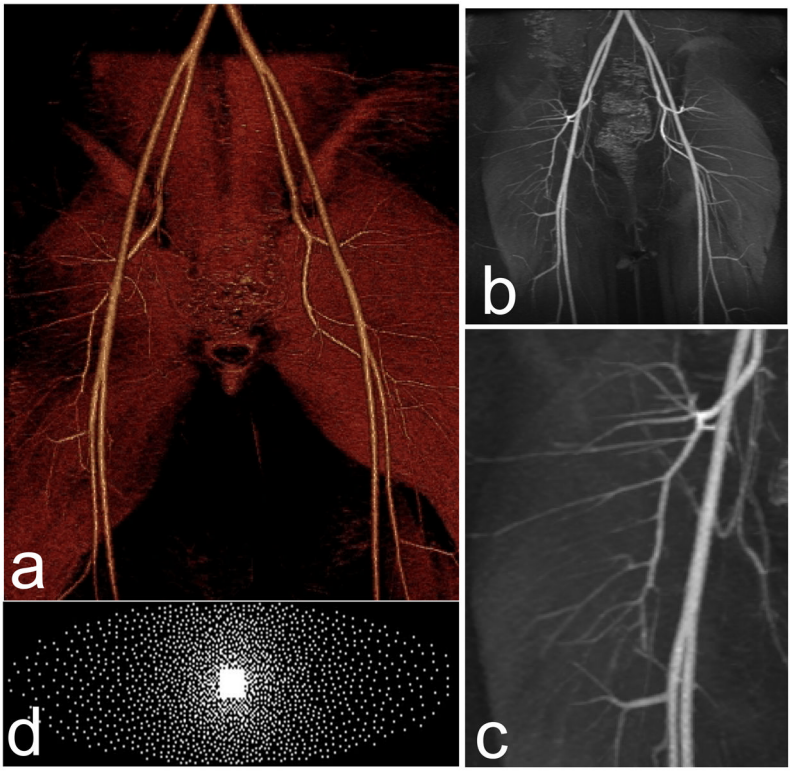

Fig. 4.

Reconstruction example with ℓ_1-SPIRiT using a dedicated 32 channel pediatric body coil. 0.875/1.6 mm in-plane/slice resolution, 8-fold accelerated acquisition of a first pass contrast MR angiography of a 6 year old patient. Pediatric patients have smaller vessels and faster circulation than adults and require much faster imaging. (a) Volume rendering (b) Maximum intensity projection (MIP) and (c) Zoomed MIP showing extraordinary level of details. (d) Our unique variable-density poisson-disc sampling pattern, optimized for CS with parallel imaging. The data was acquired within 16 seconds compared to 2 min that are required for Nyquist sampling. Due to the rapid acquisition there is no venous contamination in the image. The lack of venous contamination, along with the high SNR of the source images, enables good quality volume rendering.